AMERICAN SOCIETY FOR MICROBIOLOGY | Journal of Bacteriology®

RESEARCH ARTICLE

Roles of *Staphylococcus aureus* Mnh1 and Mnh2 Antiporters in Salt Tolerance, Alkali Tolerance, and Pathogenesis

Manisha Vaish,[a] Alexa Price-Whelan,[a]* Tamara Reyes-Robles,[b] Jun Liu,[a]* Amyeo Jereen,[a] Stephanie Christie,[a] Francis Alonzo III,[b] Meredith A. Benson,[b]* Victor J. Torres,[b] Terry A. Krulwich[a]

[a]Department of Pharmacological Sciences, Icahn School of Medicine at Mount Sinai, New York, New York, USA
[b]Department of Microbiology, NYU Langone Medical Center, New York, New York, USA

ABSTRACT *Staphylococcus aureus* has three types of cation/proton antiporters. The type 3 family includes two multisubunit Na^+/H^+ (Mnh) antiporters, Mnh1 and Mnh2. These antiporters are clusters of seven hydrophobic membrane-bound protein subunits. Mnh antiporters play important roles in maintaining cytoplasmic pH in prokaryotes, enabling their survival under extreme environmental stress. In this study, we investigated the physiological roles and catalytic properties of Mnh1 and Mnh2 in *S. aureus*. Both Mnh1 and Mnh2 were cloned separately into a pGEM3Z+ vector in the antiporter-deficient KNabc *Escherichia coli* strain. The catalytic properties of the antiporters were measured in everted (inside out) vesicles. The Mnh1 antiporter exhibited a significant exchange of Na^+/H^+ cations at pH 7.5. Mnh2 showed a significant exchange of both Na^+/H^+ and K^+/H^+ cations, especially at pH 8.5. Under elevated salt conditions, deletion of the *mnhA1* gene resulted in a significant reduction in the growth rate of *S. aureus* in the range of pH 7.5 to 9. Deletion of *mnhA2* had similar effects but mainly in the range of pH 8.5 to 9.5. Double deletion of *mnhA1* and *mnhA2* led to a severe reduction in the *S. aureus* growth rate mainly at pH values above 8.5. The effects of functional losses of both antiporters in *S. aureus* were also assessed via their support of virulence in a mouse *in vivo* infection model. Deletion of the *mnhA1* gene led to a major loss of *S. aureus* virulence in mice, while deletion of *mnh2* led to no change in virulence.

IMPORTANCE This study focuses on the catalytic properties and physiological roles of Mnh1 and Mnh2 cation/proton antiporters in *S. aureus* and their contributions under different stress conditions. The Mnh1 antiporter was found to have catalytic activity for Na^+/H^+ antiport, and it plays a significant role in maintaining halotolerance at pH 7.5 while the Mnh2 antiporter has catalytic antiporter activities for Na^+/H^+ and K^+/H^+ that have roles in both osmotolerance and halotolerance in *S. aureus*. Study of *S. aureus* with a single deletion of either *mnhA1* or *mnhA2* was assessed in an infection model of mice. The result shows that *mnhA1*, but not *mnhA2*, plays a major role in *S. aureus* virulence.

KEYWORDS multisubunit cation/proton antiporter I, *Staphylococcus aureus*, Mnh1, Mnh2, pathogenesis

Staphylococcus aureus is a commensal colonizer of 20 to 30% of healthy people as normal flora of the nasopharynx, skin, and other secondary niches (1). Colonization leads to elevated risk for metastatic *S. aureus* infections of the host. *S. aureus* strains cause a large diversity of infections (1, 2). Factors underpinning this diversity include robust stress resilience, biofilm formation, resistance to successive antibiotics, generation of antibiotic-tolerant persisters, and evasion of the host immune response (3–6). *S. aureus* not only is prevalent in hospital settings but also has survival efficiency in hostile environments. It successfully survives in high saline up to 25% NaCl, which is commonly

Received 11 October 2017 **Accepted** 8 December 2017

Accepted manuscript posted online 20 December 2017

Citation Vaish M, Price-Whelan A, Reyes-Robles T, Liu J, Jereen A, Christie S, Alonzo F, III, Benson MA, Torres VJ, Krulwich TA. 2018. Roles of *Staphylococcus aureus* Mnh1 and Mnh2 antiporters in salt tolerance, alkali tolerance, and pathogenesis. J Bacteriol 200:e00611-17. https://doi.org/10.1128/JB.00611-17.

Editor Olaf Schneewind, University of Chicago

Address correspondence to Terry A. Krulwich, terry.krulwich@mssm.edu.

* Present address: Alexa Price-Whelan, Department of Biological Sciences, Columbia University, New York, NY, USA; Jun Liu, Tianjin Institute of Industrial Biotechnology, Chinese Academy of Sciences, Tianjin Economic Area, China; Meredith A. Benson, Division of Infectious Diseases, Boston Children's Hospital, Boston, Massachusetts, USA.

found in canned foods. The low water activity (a_w) makes the bacteria uniquely resistant to drying and capable of growing and producing enterotoxins in foods with low a_w (7, 8). *S. aureus* lives in highly alkaline (pH up to 9.5) conditions that are found in garden soil, sewage, ground water, and some parts of the human gut (9, 10). Its ability to grow under osmotic and pH stress underpins the ability of *S. aureus* to thrive in a wide variety of foods, including cured meats that do not support the growth of other foodborne pathogens (11), and is responsible for staphylococcal food poisoning. Such high tolerance of salt and alkaline pH is largely due to the activity of antiporters found in the plasma membrane, which remove toxic cations from the cytoplasm and enable *S. aureus* to survive under diverse challenging conditions. *S. aureus* has three families of antiporters called cation/proton antiporters (CPA), namely, CPA1, CPA2, and CPA3. In the present study, we have focused on two homologous, multisubunit cation/proton antiporters of *S. aureus*, Mnh1 and Mnh2 of the CPA3 family. Most bacterial cation/proton antiporters are the products of single genes encoding a hydrophobic transporter that often functions as a homodimer (12, 13). In contrast, both *S. aureus* Mnh antiporters are expressed from two different operons, each of which encodes seven genes whose hydrophobic products are designated MnhA to MnhG. The single homologous operon of *Listeria monocytogenes* also has seven subunits (14), with more sequence homology to *S. aureus* Mnh1 than to Mnh2. In contrast, some bacteria, e.g., *Vibrio cholerae* and *Pseudomonas aeruginosa*, have a six-protein variation in which the first two genes are fused (15–17). Both of these hetero-oligomeric antiporter types are categorized in the cation/proton antiporter (CPA) family 3 database, Transport DB (18). These are called Mrp antiporters representing multiple resistances and pH roles (18, 19). Mrp-type antiporters were found initially in alkaliphilic *Bacillus halodurans* (20), but many nonalkaliphiles have Mrp/Mnh antiporters with roles in pH homeostasis, halotolerance, osmotolerance, and resistance to cholate (15, 21–23); *P. aeruginosa mrp* also supports pathogenesis (16).

Although the Mnh1 antiporter of *S. aureus* was among the early Mrp-type antiporters described and was shown to catalyze Na^+/H^+ antiport activity (21), its roles have not been extensively explored. An extensive study showed that *S. aureus* strains do not have complex I-type NADH oxidoreductases (24). As detailed structural information became available for a bacterial complex I (25), Mopathi and Hägerhäll (26) showed that the Mnh1 antiporter of *S. aureus* lacks features required to harness a complex I type of electron transport module. They proposed that Mrp-type antiporters are secondary antiporters that are likely progenitors of protein modules that gained the ability to partner with electron transport modules in other bacteria (27, 28). The elevated membrane potential that accompanies activity of an Mnh antiporter is explained by feedback loops. High pH or elevated cation levels increase the demand for proton motive force (PMF) to support the increased cation/proton antiport activity required for pH and/or cation homeostasis. In such instances, increased expression of electron feeders of respiratory chain and/or respiratory components themselves have been observed (29, 30). Finally, a purified Mrp homologue of Mnh antiporters was coreconstituted in proteoliposomes with an ATPase to establish a PMF and was demonstrated to be functional with no oxidoreductase activity involved (31). The Mnh1 antiporter is thus expected to function as a secondary antiporter that catalyzes PMF-dependent Na^+/H^+ antiport activity as originally suggested (21). *S. aureus* strains also have, as already noted, a second Mnh that is designated Mnh2 (17). In this study, the catalytic capacities and physiological roles of the two Mnh antiporters of *S. aureus* were examined in two *S. aureus* strains, SH1000 and Newman. Using *S. aureus* Newman, effects of functional loss of Mnh1 or Mnh2 were also assessed in a murine infection model.

RESULTS

Expression of Mnh1 is largely constitutive while Mnh2 is induced by σ^B. The two *mnh* operons of *S. aureus* are transcribed in different directions from different loci in the chromosomes. Additionally, while the *mnh1* operon consists solely of the seven *mnh1* genes, an integrase-recombinase gene (*itr*) was found to precede the seven *mnh2*

TABLE 1 Effects of selected conditions on expression of *mnh1* and *mnh2* genes, compiled from the *Staphylococcus aureus* Transcriptome Meta-Database (SATMD)

	Relative expression by condition (reference)								
Gene	Cold shock (59)	Stringent response (59)	Berberine chloride (60)	Alkali (61)[a]	Inorganic acid (61)[b]	2 M NaCl (41)	SigB (35)	Fusidic acid (62)	Biofilm vs planktonic (63)[c]
mnhA1		↓	↓	↓					
mnhB1		↓	↓						
mnhC1		↓	↓	↓					
mnhD1		↓							
mnhE1	↓	↓		↓		↓			
mnhF1		↓		↓		↓			
mnhG1		↓		↓		↓			
mnhA2	↓		↑	↑			↑		
mnhB2							↑	↑	↓
mnhC2							↑	↑	↓
mnhD2			↑	↑	↓		↑	↑	
mnhE2		↓	↑	↑	↓		↑	↑	
mnhF2		↓	↑	↑	↓		↑	↑	
mnhG2	↓	↓	↑	↑	↓			↑	

[a]Alkali, pH 10 with NaOH.
[b]At pH 4 with HCl.
[c]At an OD value of 1.0.

genes. The *S. aureus* chromosome encodes six other candidate cation/proton antiporters from three additional antiporter families (CPA1, CPA2, and NhaC). The single CPA2 family member was reported to be a receptor for signaling nucleotide c-di-AMP (32).

A survey of microarray-based gene expression experiments indicated that *mnh1* genes are relatively unresponsive to environmental changes (33) (Table 1). In contrast, the *mnh2* operon is controlled by σ^B and is upregulated under stressful conditions, with patterns that often diverge from expression patterns of *mnh1* (34, 35).

We compared expression of *mnh1* and *mnh2* operon genes in Newman and SH1000 grown in Luria-Bertani broth (LB) without added NaCl or KCl (LB0 medium) until log phase. Expression levels of the *mnh1* and *mnh2* operon genes were higher in Newman than in SH1000 (Fig. 1). These data sets were analyzed using a quantitative PCR (qPCR) assay on each of the two strains.

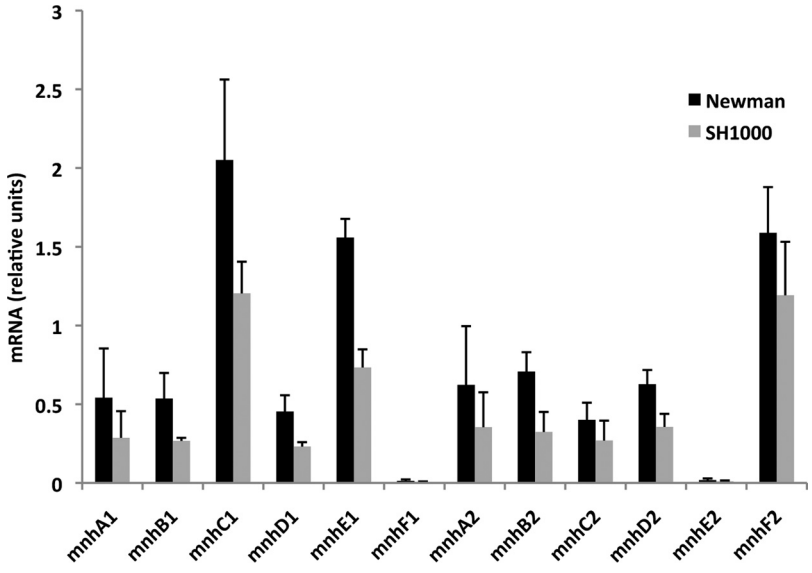

FIG 1 Expression of *mnh1* and *mnh2* operon genes in *S. aureus* Newman and SH1000 strains grown in defined LB0 medium with no added salt. Data represent the average of biological triplicates. Error bars represent standard deviations. *pyk* and *fabD* were used as a reference genes.

TABLE 2 Activity profile of Mnh1 and Mnh2[a]

Antiporter and substrate (15 mM)	Assay pH[b]	Antiport activity (% dequenching)	K_m (mM)[c]
Mnh1: Na^+	7.5	21 ± 1	0.56 ± 0.02
Mnh2			
Na^+	9.0	36 ± 1	0.30 ± 0.01
K^+	9.0	39 ± 1	0.39 ± 0.21

[a]Antiporter assays used 2.5 mM Tris-succinate as the electron donor to the respiratory chain so that a proton motive force, acidic inside, was generated across the everted membrane vesicles. The vesicles were prepared from antiporter-deficient *E. coli* KNabc transformed with a pGEM3zf+ vector into which either *mnh1* or *mnh2* was cloned along with a vector control.

[b]The antiporter assays were conducted at pH values from pH 7 to pH 9.5. The assay pH that is shown was the pH that yielded the highest activity.

[c]The K_m (±standard deviation) was calculated at the assay pH shown and is the average from three independent experiments that were conducted with duplicate assays with freshly prepared vesicles prepared from pregrown cells as described in Materials and Methods.

Comparison of catalytic properties and physiological roles of the two Mnh antiporters. Assays for Mnh antiport activity were conducted in everted (inside out) membrane vesicles of *Escherichia coli* KNabc, a cation/proton antiporter-deficient strain (Table 2). *E. coli* KNabc was transformed with either an empty control plasmid or a plasmid expressing either the *S. aureus* SH1000 *mnh1* or *mnh2* operon; raw antiporter data are shown in Fig. 2. Mnh1 catalyzed Na^+/H^+ antiport activity at a pH optimum of 7.5 but still exhibited modest antiport activity at pH 9.0. In contrast, Mnh2 catalyzed Na^+/H^+ and K^+/H^+ antiport activity, showing little Na^+/H^+ antiport and no K^+/H^+ antiport activity at pH 7.5. As the pH was increased to pH 9.0, increasing Mnh2 antiport activity was observed (Fig. 2), but although not shown, the antiport activity of Mnh2 at pH 9.5 dropped to zero. The profile shown in Table 2 includes the K_m for the antiport activities at the optimum pH for each of the two antiporters, pH 7.5 for Mnh1 and pH 9.0 for Mnh2, in the *E. coli* host used in the assay. The assays shown in Table 3 indicate that if sufficient [Na^+] is provided for Mnh2, this antiporter exhibits Na^+/H^+ antiport activity comparable to that of Mnh1 at pH 7.5, with either succinate or ATP establishing the PMF that energizes the exchange. Cytoplasmic concentrations of K^+ in the range of 900 mM are found in *S. aureus* (36), and this is sufficient to enable Mnh2 to carry out K^+/H^+ antiport activity even when the antiporter is functioning at a pH significantly below its optimal pH range (Table 3). At such a high concentration of potassium salt in the cytoplasm, the Mnh1 antiporter was inactive, which shows that Mnh2 plays a more important role in osmotolerance. In this study, we report Mnh2 antiport activity for the first time.

In order to compare the major physiological contributions of Mnh1 and Mnh2, Δ*mnhA1* and Δ*mnhA2* single deletion mutants and a double mutant with deletions in both Δ*mnhA1* and Δ*mnhA2* were constructed in *S. aureus* SH1000 and Newman. SH1000 had been used in the work that led to the proposal that Mnh was part of a PMF-generating NADH dehydrogenase (37). Deletion of the *mnhA* gene in SH1000 and Newman completely inactivated Mnh1 and Mnh2, respectively. It was noted that the Δ*mnhA1* mutant formed smaller colonies that were hyperpigmented and more orange than the colonies of the staphyloxanthin-containing wild-type strain. A Δ*mnh1* and Δ*mnh2* double mutant showed significantly more pigmentation than a Δ*mnh1* single deletion in SH1000. There was not much difference in the pigment levels of the Δ*mnh1* and Δ*mnh1* Δ*mnh2* strains in Newman (Fig. 3A). The increase in pigment is recognized as a stress response (38, 39). All the strains of SH1000, mutants and wild type, showed more pigmentation than Newman strains (Fig. 3C). The reason for more pigmentation in the SH1000 strain is overexpression of the *sigB* genes, which also regulates the stress responses. The peaks in absorbance spectra of methanol extracts of the mutant showed a slight shift relative to wild-type spectra (Fig. 3B), suggesting the presence of additional carotenoids that may include staphyloxanthin intermediates (40). No similar carotenoid elevation or shift was observed in the Δ*mnh2* mutant.

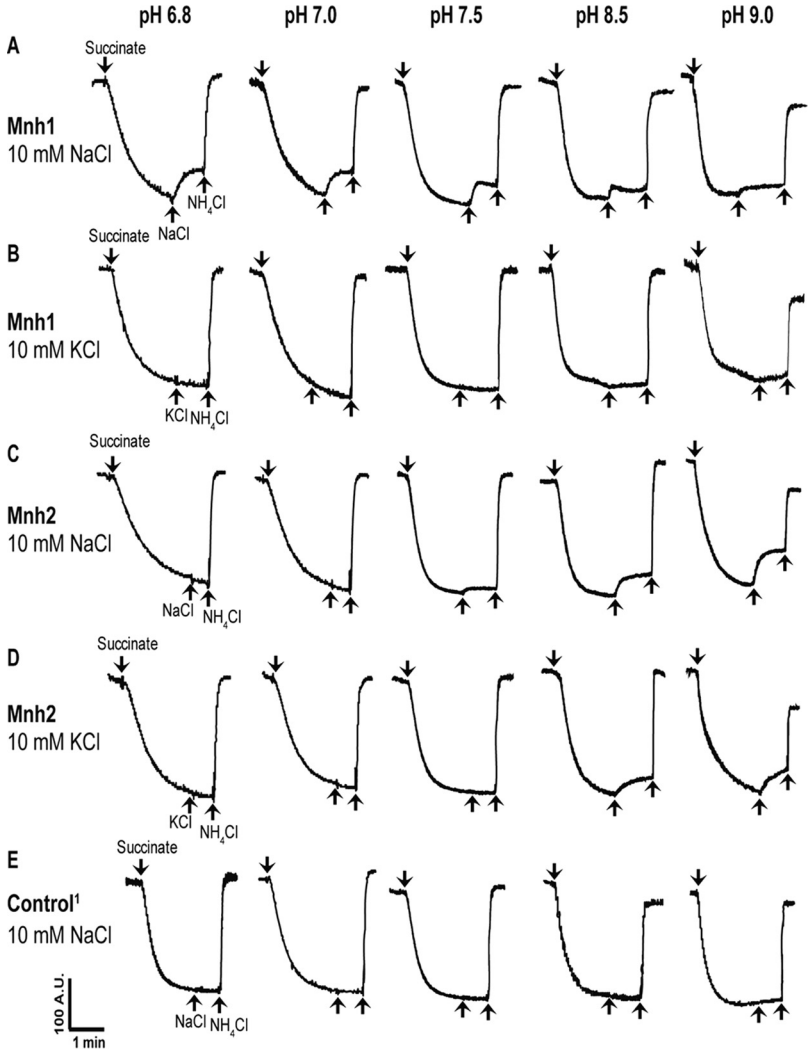

FIG 2 Antiport activity of Mnh1 and Mnh2. Mnh1 (A and B) and Mnh2 (C and D) were assayed for Na^+/H^+ and K^+/H^+ antiport activity, as a function of pH. (E) An empty vector control set of Na^+/H^+ antiport activity assays was also conducted as a function of pH. Membrane vesicles from pregrown cells were prepared in an inside out orientation relative to the cell membrane from *E. coli* KNabc cells expressing *S. aureus* SH1000 *mnh1* or *mnh2* in pGEM3zf+ vector as described earlier (57). Succinate (2.5 mM) addition initiated PMF generation, as monitored via the quenching of fluorescence of acridine orange, a ΔpH probe present at 1 μM. Antiport activity was assessed from the percent dequenching of acridine orange fluorescence after addition of 10 mM NaCl or KCl. Addition of NH_4Cl to each assay abolished residual ΔpH and established a baseline. The tracings shown are representative of assays that were carried out on at least three independent vesicle preparations, with the assays conducted in duplicate for each preparation. A.U., arbitrary units. An empty-vector control set of K^+/H^+ antiporter assays was also conducted and resulted in no dequenching with KCl addition (data not shown).

To further explore the roles of the two Mnh antiporters in *S. aureus* physiology, we studied these antiporters in the commonly used methicillin-susceptible *S. aureus* strains Newman and SH1000. Growth experiments were conducted in LB0 medium, with no addition of sodium or potassium to the base medium (LB0). As determined by flame photometry, the sodium concentration in LB0 medium was 14.1 mM, and the potassium concentration was 7.3 mM (41).

None of the mutants, not even the Δ*mnhA1* Δ*mnhA2* mutant, showed a growth defect in LB0 medium at pH 7.5 without added salt, whereas addition of 1 M NaCl resulted in a significant growth defect in the Δ*mnhA1* strain and no growth for the double mutant (Fig. 4). Increased pH exacerbated the growth defects both with and without added sodium. No obvious role for the Mnh2 antiporter was observed in

TABLE 3 Mnh1 and Mnh2 antiport activities at pH 7.5[a]

Antiporter and substrate	Concn (mM)	Antiport activity (% dequenching)[b]	
		Succinate	ATP
Mnh1: Na^+	15	21 ± 1	24 ± 1
Mnh2			
Na^+	600	27 ± 2	28 ± 1
K^+	900	28 ± 3	37 ± 1

[a]Antiporter assays were conducted at pH 7.5 using the concentrations of Na^+ or K^+ indicated, which were determined in preliminary experiments not shown. The efficacies of Tris-succinate and Tris-ATP in providing energy for proton motive force (PMF) generation were compared in each of the duplicate assays conducted in three independent experiments using freshly prepared vesicles from cells that were pregrown as described in Materials and Methods.

[b]Succinate generates PMF by donating electrons to the electron transport chain of the antiporter-deficient *E. coli* KNabc host, while ATP generates PMF by powering the *E. coli* KNabc F_1F_o-ATPase, which directly pumps protons inward in the everted membrane vesicle system.

coping with addition of 1 M NaCl at pH 7.5 or 8.5 except that the double mutant exhibited a growth deficit relative to the growth of the Δ*mnhA1* single mutant at pH 8.5. When 1 M KCl was added instead, no significant defect was observed in the Δ*mnhA2* mutant at pH 7.5, but at pH 8.5 there was a significant growth deficit, with the single mutant being almost as impaired as the double mutant. In general, the Δ*mnhA1* mutant exhibited less growth inhibition in response to added 1 M KCl than to 1 M NaCl, and the Δ*mnhA2* mutant exhibited less growth inhibition in response to added 1 M NaCl than to 1 M KCl. The results were consistent with distinct but partially overlapping roles of the two Mnh antiporters. The Δ*mnhA1*, Δ*mnhA2*, and Δ*mnhA1* Δ*mnhA2* mutant strains were more sensitive to salt and pH stress in the Newman than in the SH1000 background.

The growth patterns of wild-type *S. aureus* Newman were compared to those of mutants lacking Mnh1 or Mnh2 activity (Δ*mnhA1* or Δ*mnhA2* strain). Even in the absence of added Na^+, there was some growth inhibition of the Δ*mnhA1* mutant strain but not of the Δ*mnhA2* mutant strain (Fig. 4). In the presence of 2 M NaCl at pH 7.5, the Δ*mnhA1* mutant exhibited no growth whereas growth of the Δ*mnhA2* strain was unaffected. In the presence of 2 M KCl at pH 7.5, both the Δ*mnhA1* and the Δ*mnhA2* mutants showed significant growth defects, with the Δ*mnhA1* mutant exhibiting a more severe defect than the Δ*mnhA2* mutant. Plasmid-based complementation re-

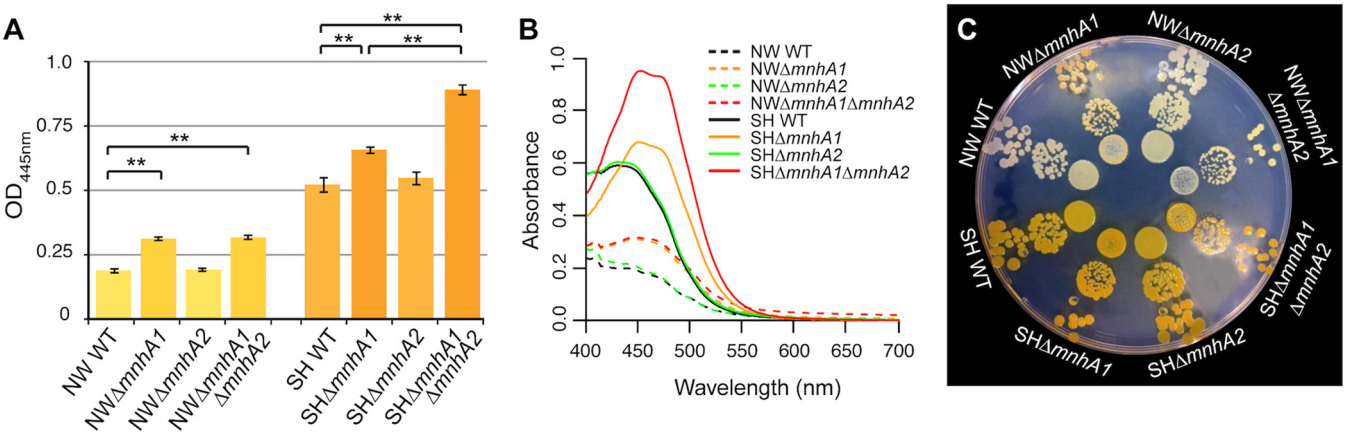

FIG 3 Carotenoid changes observed in single and double mutants of *S. aureus* SH1000 and Newman relative to levels in the wild type. (A) Carotenoid measurements for *S. aureus* SH1000 and Newman wild-type, Δ*mnhA1*, Δ*mnh2*, and Δ*mnh1* Δ*mnh2* strains. (B) Sample absorbance spectra for methanol extracts of *S. aureus* SH1000 and Newman wild-type and Δ*mnhA1*, Δ*mnhA2*, and Δ*mnhA1* Δ*mnhA2* strains. (C) Radial plating of *S. aureus* SH1000 and Newman for carotenoid comparison between wild-type and mutant strains. **, $P < 0.01$ by unpaired *t* tests between results for the wild-type and Δ*mnhA1* strains and between results for the wild-type and Δ*mnhA1* Δ*mnhA2* strains.

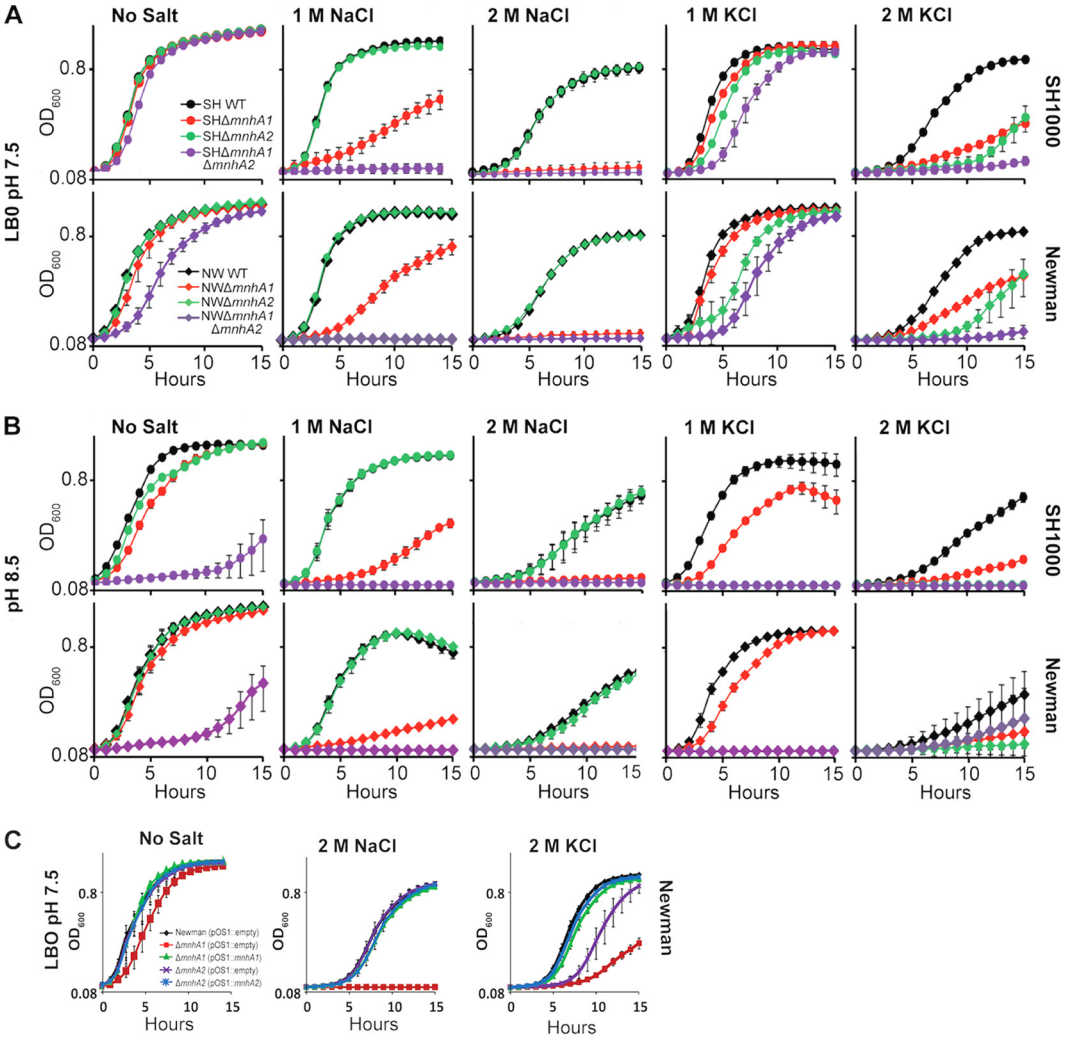

FIG 4 (A) Effects of NaCl and KCl on growth of *S. aureus* SH1000 (SH) and Newman (NW) wild-type (WT), Δ*mnhA1* and Δ*mnhA2* mutants, and the Δ*mnhA1* Δ*mnhA2* double mutant. For the experiments shown in all panels, strains were grown in LB0 medium at 37°C, pH 7.5. Additions of 1 M, 2 M NaCl, and 1 M, 2 M KCl were made, as indicated. (B) The same strains were grown as described for panel A except that the pH was 8.5. (C) For the complementation experiments, the Newman Δ*mnhA1* mutant was transformed with the pOS1 vector containing the *mnhA1* gene while the Δ*mnhA2* strain was transformed with pOS1 containing *mnhA2*. For the complementation controls, pOS1 with no insert (pOS1::empty) was transformed into each of the three strains (i.e., wild-type, Δ*mnhA1*, and Δ*mnhA2* strains). The growth curves for this and other experiments are the average of three independent experiments in which duplicate assays were conducted; the error bars represent the standard deviations.

stored the growth of these mutants to the wild-type level under the conditions tested (Fig. 4C).

All efforts to make a clean deletion of the *mnhA1* gene in naturally occurring Δ*mnh2* strains like JE2, LAC, and LAC* failed. However, when we tried to disrupt the *mnhA1* gene by introducing a chloramphenicol resistance cassette in Δ*mnhA2* Newman, we successfully obtained a double deletion of the Δ*mnh1* and Δ*mnh2* genes. JE2, LAC, and LAC* strains showed a phenotype similar to that of the SH1000 and Newman Δ*mnhA2* strains (Fig. 5).

A transposition that disrupts the *mnh2* operon is found in the *S. aureus* USA300 LAC strains in which Mnh1 was initially suggested to be essential. Fey et al. (42) reported that the *mnh*1 genes are candidates for essential genes, based on a screen that was conducted with community-acquired methicillin-resistant *S. aureus* (CA-MRSA) USA300_LAC derivatives, with the JE2 strain used for transposon mutagenesis. The USA300_FPR3757 genomic sequence (NCBI reference sequence NC_007793) was used as the reference sequence. A critical observation was the absence of some

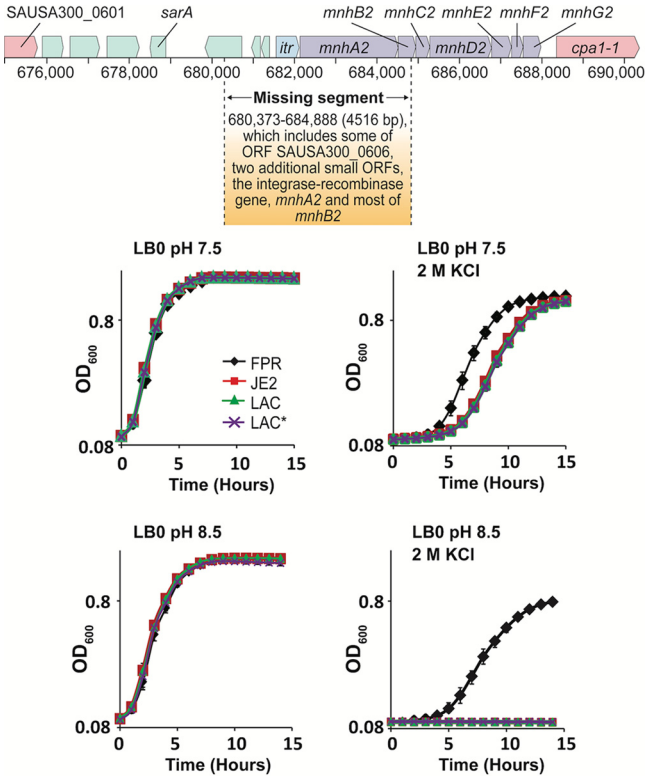

FIG 5 A partial *mnh2* deletion in *S. aureus* JE2 and two related strains leads to a growth defect at high osmolarity that is exacerbated by elevated pH. (Top) The JE2 strain and related LAC and LAC* strains were found by sequencing to have a partial *mnh2* deletion that occurred upon a transposition from another chromosomal region. The resulting deletion that includes part of the *mnh2* locus extends upstream beyond *mnh2* to several more small ORFs. This is shown diagrammatically using the numbering of *S. aureus* USA300 _FPR3757 so that the numbers up to the displacement correspond to wild-type numbering, without the effect of the deletion from the other segment that relocated. The deletion affecting *mnh2* is shown by the missing segment described in the box. (Bottom) Growth curves comparing JE2, LAC, and LAC* to growth of the reference strain, USA300_FPR3757, with and without the addition of 2 M KCl at either pH 7.5 or 8.5. The growth curves are the average of three independent experiments, with the error bars representing the standard deviations.

mnh2 genes, along with that of the *itr* gene of the *mhh2* operon and a few small unrelated genes that are usually upstream of the operon. Sequence examinations revealed that these genes were replaced during transposition of an ~13.1-kb element from another region of the genome into the region containing the *mnh2* operon. The transposition resembled but was not completely identical to a transposition reported by Highlander et al. (43) in *S. aureus* USA300-HOU-MR. We found similar insertions in additional *S. aureus* strains, with an overall frequency below 5% in the 67 strains that were examined on the NCBI site. The deletion site is shown in Fig. 5 using the framework of the USA300_FPR3757 reference strain, which has intact *mnh1* and *mnh2* operons so that the sequence numbers retain the wild-type numbering rather than reflect the downstream loss of a transposed element. Growth curves are shown for the reference wild-type strain, *S. aureus* FPR3757, and three other related strains made for various screens. JE2 is the strain into which the deletions were made in the study of Fey et al. (42), LAC is the parental strain, and LAC* is an erythromycin-sensitive version of LAC. All three strains exhibited sensitivity to 2 M KCl that was exacerbated by elevation of the pH from 7.5 to 8.5 (Fig. 4). This was consistent with loss of Mnh2 function. Multiple attempts to inactivate the intact *mnh1* locus in the JE2 and LAC strains were unsuccessful, in contrast to our success in making a double mutant in *S. aureus* SH1000 and Newman. In the JE2 and LAC strains it is possible that Mnh1 is essential. The viability of the double mutant of Newman shows that *mnh1* is not essential. The growth

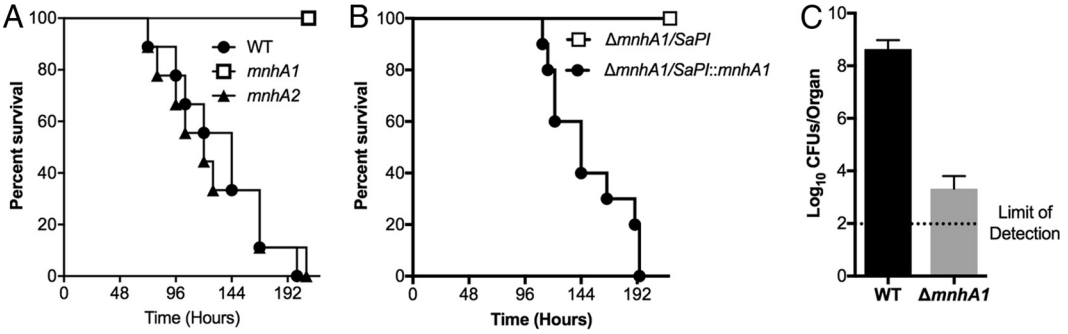

FIG 6 Mnh1 is required for *S. aureus* fitness and pathogenesis *in vivo*. (A) Survival of mice infected intravenously with ~1 × 10^7 CFU of the isogenic *S. aureus* wild-type ($n = 10$), Δ*mnhA1* ($n = 10$), or Δ*mnhA2* ($n = 10$) strain. (B) Survival of mice infected intravenously with 2 × 10^7 to 4 × 10^7 CFU of the isogenic *S. aureus* Δ*mnhA1*/SAPI (2.2 × 10^7 CFU; $n = 10$) or Δ*mnhA1*/SAPI::*mnhA1* (3.45 × 10^7 CFU; $n = 10$) strain. (C) CFU counts from kidneys isolated at the end of the experiment from mice infected with the Δ*mnhA1* strain compared to CFU counts from kidneys isolated at ~96 h postinfection with the wild-type strain. The bar indicates the median. The dotted line indicates the limit of detection.

patterns of JE2, LAC, and LAC* were similar to the growth of the Δ*mnh2* mutant strain of methicillin-sensitive Newman and SH1000.

Mnh1 is required for fitness and pathogenesis *in vivo*. To evaluate the contributions of Mnh1 and Mnh2 to *S. aureus* pathogenesis, mice were infected systematically with isogenic mutants of strain Newman lacking a functional form of either Mnh1 or Mnh2 and compared to a wild-type control with respect to their virulence. The strain with the Δ*mnhA2* deletion exhibited virulence similar to that of the wild-type strain, whereas the strain with the Δ*mnhA1* deletion showed marked attenuation of virulence (Fig. 6A). To ensure that the phenotype observed was only dependent on the lack of a functional Mnh1 antiporter, a complemented strain was generated by introducing a wild-type copy of *mnhA1* into the Δ*mnhA1* deletion mutant as a single copy inserted into the SaPI1 site in the chromosome, as had been done previously (44). Expression of the chromosomal wild-type copy of *mnhA1* reversed the virulence defect of the strain with the Δ*mnhA1* deletion (Fig. 6B). Consistent with the survival data, the Δ*mnhA1* deletion mutant exhibited an ~5-log reduction in bacterial burden in the kidneys of infected mice relative to the level with wild-type Newman (Fig. 6C).

DISCUSSION

This study confirms that both Mnh1 and Mnh2 of *S. aureus* are secondary antiporters that catalyze K^+ and/or Na^+ ion efflux in exchange for H^+ ions. The PMF provides the required energy just as well when proton pumping is energized by ATPase activity as when ion pumping via the electron transport chain is involved (Table 3). *S. aureus* strains are usually able to grow in a range of pHs from pH 5 to at least pH 9 (45) and persist at high osmolarity (41). Mnh1 and Mnh2 have important roles in halotolerance and osmotolerance, respectively (Fig. 4). Nonetheless, they have enough functional overlap that each Mnh can play a critical compensating role in viability when the other Mnh has lost function. Inactivation of Mnh1 by deletion of its first structural gene (*mnhA1*) resulted in a large reduction in the lethal effects of the wild-type strain in a murine systemic infection mode. Lethality was restored by restoration of a functional *mnhA1* into the chromosome (Fig. 6). A comparable deletion of *mnh2* in *S. aureus* Newman did not result in a virulence change. Thus, Mnh1 but not Mnh2 is of interest as a possible new target for incapacitating *S. aureus* in animal hosts. The Δ*mnh1* mutant strain is also sensitive to sucrose-generated stress that indicates the osmotolerance of Mnh1 at pH 7.5 to 8.5 (data not shown). Mnh2 would need a high concentration of cytoplasmic K^+ in order to carry out K^+/H^+ antiport activity in the nearly neutral range of pH that is optimal for Mnh1 (Table 2); this contingency is likely to be the rationale for the high cytoplasmic K^+ levels that have been found in *S. aureus* strains (36). Mnh2, which supports osmotolerance, may be a target to consider in the context of packaged-food poisoning by *S. aureus* strains.

TABLE 4 Bacterial strains and plasmids used in this study

Strain or plasmid	Description	Source or reference
Strains		
Staphylococcus aureus		
SH1000	*S. aureus* 8325-4 with repaired *rsbU*	64
SH1000 Δ*mnhA1*	Markerless deletion of the *mnhA1* gene in SH1000 (locus tag SAOUHSC_00889)	This study
SH1000 Δ*mnhA2*	Markerless deletion of the *mnhA2* gene in SH1000 (locus tag SAOUHSC_00625)	This study
SH1000 Δ*mnhA1* Δ*mnhA2*	Markerless deletion of the *mnhA1* and *mnhA2* gene in SH1000	This study
Newman	Wild type (clinical isolate)	65
Newman Δ*mnhA* (VJT39.95)	Markerless deletion of the *mnhA1* gene in Newman (locus tag NWMN_0822)	This study
Newman Δ*mnhA2*	Markerless deletion of the *mnhA2* gene in Newman (locus tag NWMN_0593)	This study
FPR3757	Wild type (USA300)	66
JE2	USA300 (derivative of LAC)	42
LAC	Wild type (USA300)	67
LAC*	USA300 (derivative of LAC)	68
RN4220	Restriction-deficient intermediate strain	69
RN9011	RN4220/pRN7023 (SaPI1 integrase, *cat194*)	44
Escherichia coli		
KNabc	Δ*nhaA* Δ*nhaB* Δ*chaA* (derived from *E. coli* TG1	70
DH5α	Transformation strain	71
DH5α-T1^R	Competent cells for site-directed mutagenesis	Invitrogen
Plasmids		
pMAD	*E.* coli/*S. aureus* shuttle vector	53
pOS1	*S. aureus* shuttle vector	72
pGEM-3Zf(+)	Derivative of the pGEM-3Z vector	Promega
pGEMMnh	pGEM-3Zf(+) containing the *mnh1* operon with putative promoter	30
pAMPW15	pGEM-3Zf(+) containing the *mnh2* operon with putative promoter	This study
pJC1112	SaPI1 attS suicide vector, erythromycin resistant (*ermC*)	73
pRN7023	SaPI1 integrase vector, chloramphenicol (*cat194*)	73

Several screens, with different methodologies (46–50), have been carried out to identify genes of diverse *S. aureus* strains that are essential for fitness in particular settings. The screens with highly stress-resistant *S. aureus* strains SH1000 and Newman have not shown an essential role for Mnh antiporter genes (47). Fey et al. (42) noted that Mrp antiporter genes of the single *Bacillus subtilis* Mrp-type antiporter are likely to be essential as they were among the genes that lacked transposon (Tn) insertions in a similar screen. However, we were able to get viable strains with a double deletion of Δ*mnh1* and Δ*mnh2* in the Newman strain that suggests that there is leeway. Similarly, a *B. subtilis* mutant with a full Δ*mrpA-mrpG* deletion and strains with individual deletions of the *B. subtilis mrp* genes have already been shown to be viable if the mutants are grown at nearly neutral pH in medium without added sodium ions (19, 51).

In the Pfam database of protein families, Mnh antiporters had, until recently, been grouped together with complex I-type proton pumps under Pfam00361 and identified as oxidored-q1m. Recently, the Pfam curators introduced a distinct Pfam00361 designation, proton_antipo_M, to accommodate Mrp-type secondary antiporters, including Mnh1 and Mnh2, which are independent antiporters that do not carry out redox reactions (52). Another point of confusion had been caused by inconsistent name assignments for the *mnh1* and *mnh2* antiporters in *S. aureus* genome annotations. A significant number of *mnh2* antiporters are annotated as *mnh1* antiporters and vice versa. This should now be easy to correct since the *mnh1* operon has only the seven structural genes, and the *mnh2* operon can thus be distinguished by its additional integrase-recombinase gene, *itr*, which precedes the *mnh2* structural genes.

MATERIALS AND METHODS

Bacterial strains and their cultures, plasmids, and primers. The bacterial strains, plasmids, and primers used in this study are listed in Tables 4 and 5.

Growth conditions. *S. aureus* strains were routinely grown in a modified version of Luria-Bertani broth (LB), designated LB0, which is LB without added NaCl or KCl. Cultures were incubated at 37°C with shaking at 225 rpm. For plasmid selection in *S. aureus* strains, erythromycin was added to the medium at 2.5 μg/ml, and chloramphenicol was added at 10 μg/ml. For growth experiments, a BioTek Power-

TABLE 5 Primers used in this study

Function (strain) and primer name[a]	Sequence
mnhA1 deletion (SH1000)	
mnhA1 del 1-1	ATAGGTACCACGCGTATTGGTCCATGTTT
mnhA1 del 1-2	TGAGTTTGTTACATATTGCGGTGGTGCTTGGTATCGCAGGATT
mnhA1 del 2-1	AATCCTGCGATACCAAGCACCACCGCAATATGTAA
mnhA1 del 2-2	ATAGGATCCCAGCCACCATCTGCAAGTT
mnhA2 deletion (SH1000)	
mnhA2 del 1-1	ATAGGATCCTGTTTCTCCAGTAAGTCGCTCA
mnhA2 del 1-2	GCTCTAAAGTCACCAAGTATCGCCGCTATGTACCCGGCATATT
mnhA2 del 2-1	AATATGCCGGGTACATAGCGGCGATACTTGGTGACTTTAGAGC
mnhA2 del 2-2	ATAGAATTCGACGGTGACGCTGAACATAA
mnhA1 deletion (Newman)	
mnh1-F1369	ATAGGATCCCCACTTTGATTTCACCTTGTTG
mnhA1 del 2-1	AATCCTGCGATACCAAGCACCACCGCAATATGTAACAAACTCA
mnh1-R4986	ATAACGCGTCAGTACCATGTTTAAGTCCGCCC
mnhA1 del 1-2	TGAGTTTGTTACATATTGCGGTGGTGCTTGGTATCGCAGGATT
mnhA2 deletion (Newman)	
mnh2-F1473	ATAGGATCCGAAGCGCTCAAGATAAAATCTG
mnhA2 del 1-2	GCTCTAAAGTCACCAAGTATCGCCGCTATGTACCC
mnh2-R4960	ATAGAATTCCCATACGTTCCCATACTCATAA
mnhA2 del 2-1	AATATGCCGGGTACATAGCGGCGATACTTGGTGACTTTAGAGC
mnhA1 deletion with CAT[b] gene (Newman)	
mnhA1.UpF_BamH1	ATATAGGATCCGTAGCTATGGTGTCACGA
mnhA1.UpR_Xho1	ATTTTCGCTCGAGTTAGAGTGCGAATATTAACGG
CatF_Xho1	ATATACTCGAGCGAAAATTGGATAAAGTGGG
CatR_kpn1	ATATAGGTACCGTACAGTCGGCATTATCTCA
mnhA1.DnF_kpn1	ACTGTACGGTACCATCGCAGGATTAGCTGTA
mnhA1.DnR_EcoR1	ATATAGAATTCGACACTAATTGCTGTGAG
qPCR on *mnh1* (SH1000)	
mnhA1 f	GCACCCGACTTAGCATTGAC
mnhA1 r	ATGACGGACAAACCAACACC
mnhB1 f	TATACACCTGGTGGCGGTTT
mnhB1 r	CGATAGGCGTCGCAATACA
mnhC1 f	GGCGGACTTAAACATGGTACTG
mnhC1 r	TAAGTGCTTGCGGGATAGGA
mnhD1 f	CCTTCTTCGTAATGGGTGTAGC
mnhD1 r	TCATGCGCTGAAAGGTTAGC
mnhE1 f	GCAGTGTTTTGGTTGTTTGTGAC
mnhE1 r	AACACTCTGTGTAAGAGGTAAACAAGAACTA
mnhF1 f	CATTAGATGCGATTGGTCTTCA
mnhF1 r	TGTTCAATCACCTTACCTTTGTCC
qPCR on *mnh2* (SH1000)	
mnhA2 f	GCGGATATGCTCAACACCAA
mnhA2 r	TCCCATGAAAAGCGCACA
mnhB2 f	CGTGTTAAGAACGGTCACGAA
mnhB2 r	CAATAAACCCACCACCAGGA
mnhC2 f	GGTTTGGGATGACTGCGTTT
mnhC2 r	CCCTTAGGCCTTCAATTTCATC
mnhD2 f	GTCATCGGCGCTATAGGTGT
mnhD2 r	CCTGCAAACGTGTTTGTTCC
mnhE2 f	ACAGGTTTTTCAGCGATGATTT
mnhE2 r	TCCAGGGTTCATATCTTTTGTTT
mnhF2 f	TCAAGGGACCTACAACAGCA
mnhF2 r	GAAACGGTGCCCATAAGT

[a]f, forward; r, reverse.
[b]CAT, chloramphenicol acetyltransferase.

Wave plate reader was used. Overnight cultures were inoculated at an initial optical density at 600 nm (OD_{600}) of 0.01 in a total of 200 μl of LB0, and 60 mM Bis-Tris propane and salt were added as indicated in the legend to Fig. 4. The cultures were adjusted to the desired pH with HCl and distributed in individual wells of 96-well plates. The plates were incubated with continuous shaking on the low setting at 37°C. The growth curves were conducted in three independent experiments in triplicate repeats.

Growth experiments. Glycerol stocks of *S. aureus* were inoculated in LB0 medium, pH 7.5, with no salt and grown for 16 h at 37°C with shaking at 225 rpm prior to growth experiments. Overnight cultures

were normalized to an OD_{600} of 0.2 with unbuffered LB0 medium, which contains no Bis-Tris propane and is not pH adjusted. Ten microliters of precultures at an OD_{600} of 0.2 was passed into 190 μl of corresponding medium in 96-well microplates for a starting OD_{600} of 0.01 for all growth conditions. Microplate lids were then carefully sealed with 1.2- by 40-cm silicone rubber tape and incubated in 37°C with shaking at 225 rpm in a BioTek PowerWave HT microplate spectrophotometer for 24 h. OD_{600} readings were collected every hour. Growth curves are averages of at least three independent experiments done in duplicate repeats.

Relative quantitation of staphyloxanthin pigment in wild-type *S. aureus* SH1000 and Newman and Δ*mnh* mutants. Staphyloxanthin was extracted from *S. aureus* cultures using methanol, and relative amounts were quantified by absorbance measurements. Cultures were inoculated at an OD_{600} of 0.01 in 50 ml of LB0 medium and incubated in a 250-ml flask at 37°C in the dark. After 48 h of incubation, 1,000 μl of culture was removed for OD_{600} measurements, and 15 ml of culture was centrifuged at 4,500 rpm for 20 min to harvest cells; the pellet was washed twice with sterile water. Excess water was removed, and 1 ml of methanol was added to each cell pellet. The pellets were vortexed to extract the pigment and incubated at 55°C for 20 min in the dark. Pellets were vortexed every 5 min and centrifuged at 4,500 rpm at 4°C after 20 min. Supernatant was collected in a glass tube. The level of carotenoid pigment was estimated quantitatively by measuring the absorbance at a 445-nm wavelength in a Shimadzu UV 1800 spectrophotometer.

Radial spot plating of *S. aureus* for carotenoid color comparison between strains. Overnight cultures were incubated at 37°C in LB0 medium, pH 7.5, with no salt and with shaking at 225 rpm. After 16 h of growth, cultures were normalized to an OD_{600} of 0.2 using LB0 medium, and then 100-fold serial dilutions were made. The following volumes and dilutions were plated on LB0 medium per radial wing from the inner ring for each strain: 5 μl of 10^{-2} dilutions, 13 μl of 10^{-4} dilutions, and 30 μl of 10^{-6} dilutions. The plate was incubated at 37°C for 42 h and left at 4°C for 24 h. After plates were warmed at room temperature, a picture was taken.

Construction of markerless deletions in *S. aureus* by allelic replacement. Deletions of target genes, which were done in frame, were generated using pMAD (53) according to previously published methods (54). Briefly, ~1-kb PCR products on either side of the sequence to be deleted were generated and fused by gene SOEing (55). The 2-kb product was ligated into pMAD and transformed into *E. coli*. After plasmid isolation and sequence verification, the construct was moved into *S. aureus* RN4220 by electroporation. After isolation from RN4220, the construct was electroporated into the target *S. aureus* strain. The plasmid was recombined into the chromosome by inoculating a liquid culture for 2 h at the permissive temperature (28°C), followed by overnight inoculation at the restrictive temperature (42°C) and plating of dilutions on LB0 agar containing erythromycin. Merodiploid clones (containing the plasmid recombined into the chromosome) were verified by PCR. To resolve the plasmid out of the chromosome and to generate candidate deletion mutants, liquid cultures of merodiploids were incubated at 28°C without selection and transferred by 1:100 dilutions for 7 days before being plated on LB0 agar. Candidate mutants were screened for loss of erythromycin resistance (confirming loss of the plasmid), and PCR and sequencing were used to confirm exclusive presence of the deleted allele.

The Newman Δ*mnhA1* Δ*mnhA2* mutant was not isolated using these methods; instead, a positive-selection method was utilized. The chloramphenicol acetyltransferase gene of 820 kb was amplified from pOS1 and ligated between the PCR products from either side of the *mnhA1* sequence to be deleted using gene SOEing (55). The 3-kb product was ligated into pMAD and transformed into *E. coli*. After plasmid isolation and sequence verification, the construct was moved into *S. aureus* RN4220 by electroporation. After isolation from RN4220, the construct was electroporated into the target *S. aureus* Newman Δ*mnhA2* strain. Subsequent steps were the same as those described above.

Complementation of markerless deletions. Plasmids for complementation of the *mnhA1* and *mnhA2* deletion mutants were constructed using the pOS1 vector. For *mnhA1* complementation, an ~3-kb product was amplified that contained *mnhA2* and the upstream open reading frame (ORF) that is predicted to encode an integrase/recombinase and to be coexpressed with the *mnh2* operon. This product also contains ~240 bp of sequence upstream of the gene for the putative integrase/recombinase that includes the binding site for σ^B, which controls *mnh2* expression (35). These products were ligated into pOS1, and the resulting plasmids were transformed into *E. coli*. After plasmid isolation and sequence verification, the constructs were moved into *S. aureus* RN4220 by electroporation. After isolation from RN4220, the constructs were electroporated into the appropriate target mutants of *S. aureus* Newman.

Preparation of total RNA and cDNA from *S. aureus* Newman and SH1000 strains and relative quantification of RNA transcripts by qPCR. RNA was prepared according to a method described previously (56). Cultures were inoculated in 50 ml of LB0 medium and grown up to an OD_{600} of 0.9 at 37°C. Eight milliliters of culture was added to 8 ml of RNA Protect bacteria reagent (Qiagen) in 50-ml sterile tubes and then vortexed immediately for 5 s and incubated at room temperature for 5 min. Cells were harvested by centrifugation (4,700 rpm, 21°C, and 10 min), the supernatant was poured off, and then the tube was inverted on paper towel for 10 s. Pellets were stored at −80°C overnight. The following day, RNA was isolated using an miRNeasy purification kit (Qiagen) for subsequent steps.

cDNA was synthesized using an iScript cDNA synthesis kit (170-8891; Bio-Rad), and each reaction was performed in a final volume using 200 ng of RNA according to the manufacturer's instructions. Relative qPCR was performed in a 384-well plate at the qPCR shared resource facility (Icahn School of Medicine at Mount Sinai, USA). Primers were designed using Primer 3 software. Reactions were set up in a total volume of 10 μl using 5 μl of cDNA (1:50 dilution) and 5 μl of master mix. Thermo cycling conditions

were as follows: 2 min at 95°C; 40 cycles of 95°C for 15 s, 55°C for 15 s, and 72°C for 30 s; a final step of 95°C for 15 s, 60°C for 15 s, and 95°C for 15 s. Samples were run in triplicate, and a no-template control and a no-reverse transcriptase control were run to ensure absence of DNA contamination. Data were analyzed using SDS, version 2.2.1, software (Applied Biosystems, USA).

Antiporter assays. Antiporter assays were conducted in everted membrane vesicles prepared from transformants of the triple antiporter-deficient *E. coli* KNabc strain expressing the empty vector, pGEM3zf+, or either the *mnh1* or *mnh2* operon. The everted membrane vesicles are oriented in such a manner that part of the membrane that is exposed outside the bacterial cells comes inside the vesicles. The transformants were grown overnight and then frozen in liquid nitrogen and stored at −80°C. Preparation of vesicles from the *E. coli* transformants was conducted using a French press as described earlier (57). The vesicles were used immediately after preparation, without being frozen. The assays also followed a protocol used earlier with the same buffer and pH conditions. Acridine orange was the ΔpH probe used, with measurements conducted using an RF-5301 PC Shimadzu spectrofluorophotometer equipped with a stirrer, with excitation at 420 nm and emission at 500 nm (both with a 10-mm slit). When the respiratory chain is energized by succinate, the respiratory chain starts pumping protons inside the vesicles (as vesicles are everted). The initiation of proton motive force generation is indicated for specific experiments.

Pathogenicity assays. (i) Generation of *mnhA1* chromosomal integration strains and growth curves for determination of their phenotypes. To generate isogenic *mnhA1* complementation strains, the entire *mnh* locus was amplified from *S. aureus* Newman genomic DNA using the oligonucleotide pair VJT1276 (5′-ATATAGGATCCTGAAGCTATATCGATTTTCACACAA-3′) and VJT1277 (5′-ATATAGGTACCAACT GCAGCAAATTGCAAAA-3′) and cloned into the integration vector pJC1112 using BamHI and KpnI restriction sites. The plasmid was transformed into *E. coli* DH5α and ampicillin resistance-selected clones. A positive recombinant clone was electroporated into RN9011 containing plasmid pRN7023 encoding the SaPI1 integrase to promote single-copy chromosomal integration into the *S. aureus* SaPI1 site (44) and was selected for erythromycin resistance, as described elsewhere (58). The SaPI1 integrated construct was then transduced into strain VJT39.95 (Newman Δ*mnhA1*) using previously published methods (58).

(ii) Generation of a pJC1112 control strain. To generate the pJC1112 (empty vector) control strain, purified plasmid from strain VJT9.54 (*E. coli* DH5α containing pJC1112) was electroporated into RN9011, followed by transduction into strain VJT39.95 (Newman Δ*mnhA1*) as described above.

(iii) Murine systemic infection. Animal infections were done according to protocols approved by the New York University School of Medicine Institutional Animal Care and Use Committee. For *in vivo* experiments, 5-week-old female ND4 Swiss Webster mice (Harlan Laboratories) were anesthetized with 250 μl of Avertin (2,2,2-tribromoethanol dissolved in *tert*-amyl-alcohol and diluted to a final concentration of 2.5% [vol/vol] in sterile saline) intraperitoneally. This was followed by retro-orbital injection of 5×10^7 CFU of wild-type *S. aureus* Newman, isogenic Newman strains with either a single *mnhA1* deletion or *mnhA2* deletion or with an isogenic Newman *mnhA1* deletion strain complemented in single copy with either the integrase-encoding empty vector pJC1112 (Δ*mnhA1*/pJC1112) or pJC1112 with *mnhA1* in the SaPI1 site (Δ*mnhA1*/pJC1112-*mnhA1*). Mice were monitored for acute infection and signs of morbidity, at which points mice were sacrificed, and survival curves were plotted over time.

ACKNOWLEDGMENTS

This work was supported by research grant R01GM028454 from the National Institute of General Medical Sciences to T.A.K. and grant R21 AI101533 from the National Institute of Allergy and Infectious Diseases to V.J.T. S.C. was supported by a Postbaccalaureate Research Education Program grant (R25GM06118). V.J.T. is a Burroughs Wellcome Fund Investigator in the Pathogenesis of Infectious Diseases.

We declare that we have no conflicts of interest.

REFERENCES

1. Fitzgerald JR. 2014. Evolution of *Staphylococcus aureus* during human colonization and infection. Infect Genet Evol 21:542–547. https://doi.org/10.1016/j.meegid.2013.04.020.
2. Uhlemann AC, Otto M, Lowy FD, DeLeo FR. 2014. Evolution of community- and healthcare-associated methicillin-resistant *Staphylococcus aureus*. Infect Genet Evol 21:563–574. https://doi.org/10.1016/j.meegid.2013.04.030.
3. Conlon BP, Rowe SE, Lewis K. 2015. Persister cells in biofilm associated infections. Adv Exp Med Biol 831:1–9. https://doi.org/10.1007/978-3-319-09782-4_1.
4. Moormeier DE, Bose JL, Horswill AR, Bayles KW. 2014. Temporal and stochastic control of *Staphylococcus aureus* biofilm development. mBio 5:e01341-14. https://doi.org/10.1128/mBio.01341-14.
5. Prax M, Bertram R. 2014. Metabolic aspects of bacterial persisters. Front Cell Infect Microbiol 4:148. https://doi.org/10.3389/fcimb.2014.00148.
6. Pauli NT, Kim HK, Falugi F, Huang M, Dulac J, Henry Dunand C, Zheng NY, Kaur K, Andrews SF, Huang Y, DeDent A, Frank KM, Charnot-Katsikas A, Schneewind O, Wilson PC. 2014. *Staphylococcus aureus* infection induces protein A-mediated immune evasion in humans. J Exp Med 211:2331–2339. https://doi.org/10.1084/jem.20141404.
7. Wu X, Su YC. 2014. Effects of frozen storage on survival of *Staphylococcus aureus* and enterotoxin production in precooked tuna meat. J Food Sci 79:M1554-9. https://doi.org/10.1111/1750-3841.12530.
8. Mansfield JM, Farkas G, Wieneke AA, Gilbert RJ. 1983. Studies on the growth and survival of *Staphylococcus aureus* in corned beef. J Hyg (Lond) 91:467–478. https://doi.org/10.1017/S0022172400060514.
9. Chao WL, Ding RJ, Chen RS. 1987. Survival of pathogenic bacteria in environmental microcosms. Zhonghua Min Guo Wei Sheng Wu Ji Mian Yi Xue Za Zhi 20:339–348.
10. Aslam S, Sajid I. 2016. Antimicrobial potential of halophilic actinomycetes against multi drug resistant (MDR) ventilator associated pneumonia causing bacterial pathogens. Pak J Pharm Sci 29:367–374.
11. Cruz J, Montville TJ. 2008. Influence of nisin on the resistance of *Bacillus anthracis* Sterne spores to heat and hydrostatic pressure. J Food Prot 71:196–199. https://doi.org/10.4315/0362-028X-71.1.196.
12. Gerchman Y, Rimon A, Venturi M, Padan E. 2001. Oligomerization of

NhaA, the Na^+/H^+ antiporter of *Escherichia coli* in the membrane and its functional and structural consequences. Biochemistry 40:3403–3412. https://doi.org/10.1021/bi002669o.
13. Lee C, Kang HJ, von Ballmoos C, Newstead S, Uzdavinys P, Dotson DL, Iwata S, Beckstein O, Cameron AD, Drew D. 2013. A two-domain elevator mechanism for sodium/proton antiport. Nature 501:573–577. https://doi.org/10.1038/nature12484.
14. Bergholz TM, Bowen B, Wiedmann M, Boor KJ. 2012. *Listeria monocytogenes* shows temperature-dependent and -independent responses to salt stress, including responses that induce cross-protection against other stresses. Appl Environ Microbiol 78:2602–2612. https://doi.org/10.1128/AEM.07658-11.
15. Dzioba-Winogrodzki J, Winogrodzki O, Krulwich TA, Boin MA, Hase CC, Dibrov P. 2009. The *Vibrio cholerae* Mrp system: cation/proton antiport properties and enhancement of bile salt resistance in a heterologous host. J Mol Microbiol Biotechnol 16:176–186. https://doi.org/10.1159/000119547.
16. Kosono S, Haga K, Tomizawa R, Kajiyama Y, Hatano K, Takeda S, Wakai Y, Hino M, Kudo T. 2005. Characterization of a multigene-encoded sodium/hydrogen antiporter (Sha) from *Pseudomonas aeruginosa*: its involvement in pathogenesis. J Bacteriol 187:5242–5248. https://doi.org/10.1128/JB.187.15.5242-5248.2005.
17. Swartz TH, Ikewada S, Ishikawa O, Ito M, Krulwich TA. 2005. The Mrp system: a giant among monovalent cation/proton antiporters? Extremophiles 9:345–354. https://doi.org/10.1007/s00792-005-0451-6.
18. Ren Q, Chen K, Paulsen IT. 2007. TransportDB: a comprehensive database resource for cytoplasmic membrane transport systems and outer membrane channels. Nucleic Acids Res 35:D274–D279. https://doi.org/10.1093/nar/gkl925.
19. Ito M, Guffanti AA, Oudega B, Krulwich TA. 1999. *mrp*, a multigene, multifunctional locus in *Bacillus subtilis* with roles in resistance to cholate and to Na^+ and in pH homeostasis. J Bacteriol 181:2394–2402.
20. Hamamoto T, Hashimoto M, Hino M, Kitada M, Seto Y, Kudo T, Horikoshi K. 1994. Characterization of a gene responsible for the Na^+/H^+ antiporter system of alkalophilic *Bacillus* species strain C-125. Mol Microbiol 14:939–946. https://doi.org/10.1111/j.1365-2958.1994.tb01329.x.
21. Hiramatsu T, Kodama K, Kuroda T, Mizushima T, Tsuchiya T. 1998. A putative multisubunit Na^+/H^+ antiporter from *Staphylococcus aureus*. J Bacteriol 180:6642–6648.
22. Jasso-Chavez R, Diaz-Perez C, Rodriguez-Zavala JS, Ferry JG. 2017. Functional role of MrpA in the MrpABCDEFG Na^+/H^+ antiporter complex from the archaeon *Methanosarcina acetivorans*. J Bacteriol 199:e00662-16. https://doi.org/10.1128/JB.00662-16.
23. Meng L, Meng F, Zhang R, Zhang Z, Dong P, Sun K, Chen J, Zhang W, Yan M, Li J, Abdel-Motaal H, Jiang J. 2017. Characterization of a novel two-component $Na^+(Li^+, K^+)/H^+$ antiporter from *Halomonas zhaodongensis*. Sci Rep 7:4221. https://doi.org/10.1038/s41598-017-04236-0.
24. Spero MA, Aylward FO, Currie CR, Donohue TJ. 2015. Phylogenomic analysis and predicted physiological role of the proton-translocating NADH:quinone oxidoreductase (complex I) across bacteria. mBio 6:e00389-15. https://doi.org/10.1128/mBio.00389-15.
25. Sazanov LA. 2015. A giant molecular proton pump: structure and mechanism of respiratory complex I. Nat Rev Mol Cell Biol 16:375–388. https://doi.org/10.1038/nrm3997.
26. Moparthi VK, Hagerhall C. 2011. The evolution of respiratory chain complex I from a smaller last common ancestor consisting of 11 protein subunits. J Mol Evol 72: 484–497. https://doi.org/10.1007/s00239-011-9447-2.
27. Marreiros BC, Batista AP, Duarte AM, Pereira MM. 2013. A missing link between complex I and group 4 membrane-bound [NiFe] hydrogenases. Biochim Biophys Acta 1827:198–209. https://doi.org/10.1016/j.bbabio.2012.09.012.
28. Mayer S, Steffen W, Steuber J, Gotz F. 2015. The *Staphylococcus aureus* NuoL-like protein MpsA contributes to the generation of membrane potential. J Bacteriol 197:794–806. https://doi.org/10.1128/JB.02127-14.
29. Swartz TH, Ito M, Hicks DB, Nuqui M, Guffanti AA, Krulwich TA. 2005. The Mrp Na^+/H^+ antiporter increases the activity of the malate:quinone oxidoreductase of an *Escherichia coli* respiratory mutant. J Bacteriol 187:388–391. https://doi.org/10.1128/JB.187.1.388-391.2005.
30. Swartz TH, Ito M, Ohira T, Natsui S, Hicks DB, Krulwich TA. 2007. Catalytic properties of *Staphylococcus aureus* and Bacillus members of the secondary cation/proton antiporter-3 (Mrp) family are revealed by an optimized assay in an *Escherichia coli* host. J Bacteriol 189:3081–3090. https://doi.org/10.1128/JB.00021-07.
31. Morino M, Suzuki T, Ito M, Krulwich TA. 2014. Purification and functional reconstitution of a seven-subunit mrp-type Na^+/H^+ antiporter. J Bacteriol 196:28–35. https://doi.org/10.1128/JB.01029-13.
32. Corrigan RM, Campeotto I, Jeganathan T, Roelofs KG, Lee VT, Grundling A. 2013. Systematic identification of conserved bacterial c-di-AMP receptor proteins. Proc Natl Acad Sci U S A 110:9084–9089. https://doi.org/10.1073/pnas.1300595110.
33. Nagarajan V, Elasri MO. 2007. SAMMD: *Staphylococcus aureus* microarray meta-database. BMC Genomics 8:351. https://doi.org/10.1186/1471-2164-8-351.
34. Bischoff M, Dunman P, Kormanec J, Macapagal D, Murphy E, Mounts W, Berger-Bachi B, Projan S. 2004. Microarray-based analysis of the *Staphylococcus aureus* σ^B regulon. J Bacteriol 186:4085–4099. https://doi.org/10.1128/JB.186.13.4085-4099.2004.
35. Pane-Farre J, Jonas B, Forstner K, Engelmann S, Hecker M. 2006. The σ^B regulon in *Staphylococcus aureus* and its regulation. Int J Med Microbiol 296:237–258. https://doi.org/10.1016/j.ijmm.2005.11.011.
36. Christian JH, Waltho JA. 1961. The sodium and potassium content of non-halophilic bacteria in relation to salt tolerance. J Gen Microbiol 25:97–102. https://doi.org/10.1099/00221287-25-1-97.
37. Bayer AS, McNamara P, Yeaman MR, Lucindo N, Jones T, Cheung AL, Sahl HG, Proctor RA. 2006. Transposon disruption of the complex I NADH oxidoreductase gene (*snoD*) in *Staphylococcus aureus* is associated with reduced susceptibility to the microbicidal activity of thrombin-induced platelet microbicidal protein 1. J Bacteriol 188:211–222. https://doi.org/10.1128/JB.188.1.211-222.2006.
38. Clauditz A, Resch A, Wieland KP, Peschel A, Gotz F. 2006. Staphyloxanthin plays a role in the fitness of *Staphylococcus aureus* and its ability to cope with oxidative stress. Infect Immun 74:4950–4953. https://doi.org/10.1128/IAI.00204-06.
39. Liu CI, Liu GY, Song Y, Yin F, Hensler ME, Jeng WY, Nizet V, Wang AH, Oldfield E. 2008. A cholesterol biosynthesis inhibitor blocks *Staphylococcus aureus* virulence. Science 319:1391–1394. https://doi.org/10.1126/science.1153018.
40. Marshall JH, Wilmoth GJ. 1981. Pigments of *Staphylococcus aureus*, a series of triterpenoid carotenoids. J Bacteriol 147:900–913.
41. Price-Whelan A, Poon CK, Benson MA, Eidem TT, Roux CM, Boyd JM, Dunman PM, Torres VJ, Krulwich TA. 2013. Transcriptional profiling of *Staphylococcus aureus* during growth in 2 M NaCl leads to clarification of physiological roles for Kdp and Ktr K^+ uptake systems. mBio 4:e00407-13. https://doi.org/10.1128/mBio.00407-13.
42. Fey PD, Endres JL, Yajjala VK, Widhelm TJ, Boissy RJ, Bose JL, Bayles KW. 2013. A genetic resource for rapid and comprehensive phenotype screening of nonessential *Staphylococcus aureus* genes. MBio 4:e00537-12. https://doi.org/10.1128/mBio.00537-12.
43. Highlander SK, Hultén KG, Qin X, Jiang H, Yerrapragada S, Mason EO, Jr, Shang Y, Williams TM, Fortunov RM, Liu Y, Igboeli O, Petrosino J, Tirumalai M, Uzman A, Fox GE, Cardenas AM, Muzny DM, Hemphill L, Ding Y, Dugan S, Blyth PR, Buhay CJ, Dinh HH, Hawes AC, Holder M, Kovar CL, Lee SL, Liu W, Nazareth LV, Wang Q, Zhou J, Kaplan SL, Weinstock GM. 2007. Subtle genetic changes enhance virulence of methicillin resistant and sensitive Staphylococcus aureus. BMC Microbiol 7:99. https://doi.org/10.1186/1471-2180-7-99.
44. Ruzin A, Lindsay J, Novick RP. 2001. Molecular genetics of SaPI1—a mobile pathogenicity island in *Staphylococcus aureus*. Mol Microbiol 41:365–377. https://doi.org/10.1046/j.1365-2958.2001.02488.x.
45. Kuroda M, Ohta T, Hayashi H. 1995. Isolation and the gene cloning of an alkaline shock protein in methicillin resistant *Staphylococcus aureus*. Biochem Biophys Res Commun 207:978–984. https://doi.org/10.1006/bbrc.1995.1281.
46. Bae T, Banger AK, Wallace A, Glass EM, Aslund F, Schneewind O, Missiakas DM. 2004. *Staphylococcus aureus* virulence genes identified by bursa aurealis mutagenesis and nematode killing. Proc Natl Acad Sci U S A 101:12312–12317. https://doi.org/10.1073/pnas.0404728101.
47. Chaudhuri RR, Allen AG, Owen PJ, Shalom G, Stone K, Harrison M, Burgis TA, Lockyer M, Garcia-Lara J, Foster SJ, Pleasance SJ, Peters SE, Maskell DJ, Charles IG. 2009. Comprehensive identification of essential *Staphylococcus aureus* genes using transposon-mediated differential hybridisation (TMDH). BMC Genomics 10:291. https://doi.org/10.1186/1471-2164-10-291.
48. Christiansen MT, Kaas RS, Chaudhuri RR, Holmes MA, Hasman H, Aarestrup FM. 2014. Genome-wide high-throughput screening to investigate essential genes involved in methicillin-resistant *Staphylococcus aureus* sequence type 398 survival. PLoS One 9:e89018. https://doi.org/10.1371/journal.pone.0089018.

49. Ji Y, Zhang B, Van SF, Horn Warren P, Woodnutt G, Burnham MK, Rosenberg M. 2001. Identification of critical *Staphylococcal* genes using conditional phenotypes generated by antisense RNA. Science 293:2266–2269. https://doi.org/10.1126/science.1063566.
50. Valentino MD, Foulston L, Sadaka A, Kos VN, Villet RA, Santa Maria J, Jr, Lazinski DW, Camilli A, Walker S, Hooper DC, Gilmore MS. 2014. Genes contributing to Staphylococcus aureus fitness in abscess- and infection-related ecologies. mBio 5:e01729-14. https://doi.org/10.1128/mBio.01729-14.
51. Ito M, Guffanti AA, Wang W, Krulwich TA. 2000. Effects of nonpolar mutations in each of the seven *Bacillus subtilis mrp* genes suggest complex interactions among the gene products in support of Na^+ and alkali but not cholate resistance. J Bacteriol 182:5663–5670. https://doi.org/10.1128/JB.182.20.5663-5670.2000.
52. Finn RD, Bateman A, Clements J, Coggill P, Eberhardt RY, Eddy SR, Heger A, Hetherington K, Holm L, Mistry J, Sonnhammer EL, Tate J, Punta M. 2014. Pfam: the protein families database. Nucleic Acids Res 42:D222–D230. https://doi.org/10.1093/nar/gkt1223.
53. Arnaud M, Chastanet A, Debarbouille M. 2004. New vector for efficient allelic replacement in naturally nontransformable, low-GC-content, gram-positive bacteria. Appl Environ Microbiol 70:6887–6891. https://doi.org/10.1128/AEM.70.11.6887-6891.2004.
54. Memmi G, Filipe SR, Pinho MG, Fu Z, Cheung A. 2008. *Staphylococcus aureus* PBP4 is essential for beta-lactam resistance in community-acquired methicillin-resistant strains. Antimicrob Agents Chemother 52:3955–3966. https://doi.org/10.1128/AAC.00049-08.
55. Horton RM. 1993. In vitro recombination and mutagenesis of DNA: SOEing together tailor-made genes. Methods Mol Biol 15:251–261.
56. Liu J, Ryabichko S, Bogdanov M, Fackelmayer OJ, Dowhan W, Krulwich TA. 2014. Cardiolipin is dispensable for oxidative phosphorylation and non-fermentative growth of alkaliphilic *Bacillus pseudofirmus* OF4. J Biol Chem 289:2960–2971. https://doi.org/10.1074/jbc.M113.536193.
57. Morino M, Natsui S, Swartz TH, Krulwich TA, Ito M. 2008. Single gene deletions of *mrpA* to *mrpG* and *mrpE* point mutations affect activity of the Mrp Na^+/H^+ antiporter of alkaliphilic *Bacillus* and formation of hetero-oligomeric Mrp complexes. J Bacteriol 190:4162–4172. https://doi.org/10.1128/JB.00294-08.
58. Alonzo F, III, Benson MA, Chen J, Novick RP, Shopsin B, Torres VJ. 2012. *Staphylococcus aureus* leucocidin ED contributes to systemic infection by targeting neutrophils and promoting bacterial growth *in vivo*. Mol Microbiol 83:423–435. https://doi.org/10.1111/j.1365-2958.2011.07942.x.
59. Anderson KL, Roberts C, Disz T, Vonstein V, Hwang K, Overbeek R, Olson PD, Projan SJ, Dunman PM. 2006. Characterization of the Staphylococcus aureus heat shock, cold shock, stringent, and SOS responses and their effects on log-phase mRNA turnover. J Bacteriol 188:6739–6756. https://doi.org/10.1128/JB.00609-06.
60. Wang D, Yu L, Xiang H, Fan J, He L, Guo N, Feng H, Deng X. 2008. Global transcriptional profiles of *Staphylococcus aureus* treated with berberine chloride. FEMS Microbiol Lett 279:217–225. https://doi.org/10.1111/j.1574-6968.2007.01031.x.
61. Anderson KL, Roux CM, Olson MW, Luong TT, Lee CY, Olson R, Dunman PM. 2010. Characterizing the effects of inorganic acid and alkaline shock on the Staphylococcus aureus transcriptome and messenger RNA turnover. FEMS Immunol Med Microbiol 60:208–250. https://doi.org/10.1111/j.1574-695X.2010.00736.x.
62. Delgado A, Zaman S, Muthaiyan A, Nagarajan V, Elasri MO, Wilkinson BJ, Gustafson JE. 2008. The fusidic acid stimulon of Staphylococcus aureus. J Antimicrob Chemother 62:1207–1214. https://doi.org/10.1093/jac/dkn363.
63. Beenken KE, Dunman PM, McAleese F, Macapagal D, Murphy E, Projan SJ, Blevins JS, Smeltzer MS. 2004. Global gene expression in *Staphylococcus aureus* biofilms. J Bacteriol 186:4665–4684. https://doi.org/10.1128/JB.186.14.4665-4684.2004.
64. Horsburgh MJ, Aish JL, White IJ, Shaw L, Lithgow JK, Foster SJ. 2002. σ^B Modulates virulence determinant expression and stress resistance: characterization of a functional *rsbU* strain derived from *Staphylococcus aureus* 8325-4. J Bacteriol 184:5457–5467. https://doi.org/10.1128/JB.184.19.5457-5467.2002.
65. Duthie ES, Lorenz LL. 1952. Staphylococcal coagulase; mode of action and antigenicity. J Gen Microbiol 6:95–107.
66. Diep BA, Gill SR, Chang RF, Phan TH, Chen JH, Davidson MG, Lin F, Lin J, Carleton HA, Mongodin EF, Sensabaugh GF, Perdreau-Remington F. 2006. Complete genome sequence of USA300, an epidemic clone of community-acquired methicillin-resistant *Staphylococcus aureus*. Lancet 367:731–739. https://doi.org/10.1016/S0140-6736(06)68231-7.
67. McDougal LK. 2003. Pulsed-field gel electrophoresis typing of oxacillin-resistant *Staphylococcus aureus* isolates from the United States: establishing a national database. J Clin Microbiol 41:5113–5120. https://doi.org/10.1128/JCM.41.11.5113-5120.2003.
68. Boles BR, Thoendel M, Roth AJ, Horswill AR. 2010. Identification of genes involved in polysaccharide-independent Staphylococcus aureus biofilm formation. PLoS One 5:e10146. https://doi.org/10.1371/journal.pone.0010146.
69. Novick RP. 1991. Genetic systems in staphylococci. Methods Enzymol 204:587–636. https://doi.org/10.1016/0076-6879(91)04029-N.
70. Nozaki K, Inaba K, Kuroda T, Tsuda M, Tsuchiya T 1996. Cloning and sequencing of the gene for Na^+/H^+ antiporter of Vibrio parahaemolyticus. Biochem Biophys Res Commun 222:774–779. https://doi.org/10.1006/bbrc.1996.0820.
71. Hanahan D. 1985. Techniques for transformation of *E. coli*, p 109–135. *In* Glover DM (ed), DNA cloning: a practical approach, vol. 1. IRL Press, Washington, DC.
72. Simonet JM, Boccard F, Pernodet JL, Gagnat J, Guérineau M. 1987. Excision and integration of a self-transmissible replicon of Streptomyces ambofaciens. Gene 59:137–144. https://doi.org/10.1016/0378-1119(87)90274-5.
73. Chen J, Yoong P, Ram G, Torres VJ, Novick RP. 2014. Single-copy vectors for integration at the SaPI1 attachment site for Staphylococcus aureus. Plasmid 76:1–7. https://doi.org/10.1016/j.plasmid.2014.08.001.